



Renewables power limit calculation using Monte Carlo simulation

Cálculo del límite de potencia renovable mediante simulación Monte Carlo

Moises Ferrer-Vallin^{1,*}, Pablo Sánchez Yáñez^{II}, Ariel Santos-Fuentefría^I

^IUniversidad Tecnológica de la Habana, José Antonio Echeverría, La Habana, Cuba

^{II}Unión Eléctrica, La Habana, Cuba

*Autor de correspondencia: moisesfv@electrica.cujae.edu.cu

Received: 7 de octubre de 2022

Approved: 7 de noviembre de 2022

Este documento posee una [licencia Creative Commons Reconocimiento-No Comercial 4.0 internacional](https://creativecommons.org/licenses/by-nc/4.0/)



RESUMEN/ABSTRACT

Introducing renewable non-dispatchable energy sources such as wind and solar (PV) into a power system can cause frequency deviation problems in steady-state operation scenarios. These problems are mainly related to their inherent variability and the characteristics of the grid they are connected to. These problems can be amplified in isolated power systems. This research consists in calculating the maximum value of wind and solar PV that can be connected in an isolated power system while maintaining the frequency deviation values within standard limits. An algorithm based in Monte Carlo simulations was developed to fulfil this objective. The results obtained using the described algorithm show that, in an isolated power system, renewable power values increase, frequency deviations also increase, eventually failing to comply with grid code regulations. Results also show that introducing a properly sized energy storage helps decreasing out-of-limits frequency deviations, complying with the grid code regulations.

Keywords: wind power, photovoltaic power, frequency deviation, Monte Carlo simulations.

La introducción de fuentes renovables de energía no despachables como la energía eólica y la energía solar fotovoltaica puede causar problemas de desviación de frecuencia en escenarios en estado estacionario. Estos problemas se deben principalmente a su variabilidad inherente y las características de la red a la que se conectan y pueden empeorar en redes aisladas. Este trabajo consiste en el cálculo del valor máximo de energía eólica y solar fotovoltaica que se puede conectar en un sistema aislado manteniendo los valores de desviación de la frecuencia dentro de los límites establecidos. Para lograr este objetivo se desarrolló un algoritmo basado en simulaciones Monte Carlo. Los resultados obtenidos con la utilización de este algoritmo muestran que en un sistema aislado un incremento de la penetración de renovables causa un incremento en las desviaciones de frecuencia llevando al sistema a no cumplir con los límites establecidos. Los resultados también muestran que la introducción de un sistema de almacenamiento, debidamente calculado, ayuda a reducir las desviaciones de frecuencia y cumplir con las regulaciones.

Palabras clave: energía eólica, energía solar fotovoltaica, desviación de la frecuencia, simulaciones Monte Carlo.

INTRODUCTION

In order to reduce the use of fossil fuels more renewable energy sources (RES), wind and photovoltaic (PV) power, are being used. By the end of 2020 up to 29% of the energy consumed in the world was produced using renewable energy sources. Photovoltaic was the biggest contributor with a growth of over 50%, followed by wind power with a 36% growth [1]. In order to operate a power system correctly, the grid's frequency must be maintained at a near-constant value. To efficiently control the power system's operation, the demand's behavior must be studied as, for example, the load's peaks and valleys can vary appreciably as seasons change.

How to cite this article:

Moises Ferrer Vallin, Ariel Santos Fuentefría and Pablo Sánchez Yáñez. Renewables power limit calculation using Monte Carlo simulation. Ingeniería Energética. 2022. 43(3), septiembre/diciembre. ISSN: 1815-5901.

Sitio de la revista: <https://rie.cujae.edu.cu/index.php/RIE/index>

Also, workdays and holidays can have very different demand curves. With this information and knowing the number of generators capable of frequency regulation, the upper and lower frequency variation limits can be known. Large frequency deviations can cause stress-producing vibrations in the steam turbines that power electric generators shortening the time between maintenance periods. They may also affect the efficiency of induction motors [2]. Integrating RES, such as wind and PV power, into power systems can cause frequency stability issues. The main challenges rely on their intermittency, variability and uncertainty due to their dependency on weather conditions [3]. As the wind and PV power penetration increases, frequency deviations also increase. If the amount of wind and PV power generation is above the power system's penetration limit the grid may lose its stability either partially or totally, affecting the quality of the end-consumer service and causing blackouts [4]. In some cases, to avoid a system collapse wind power generation is capped [5, 6]. The integration of RES into power systems are regulated by the grid codes [7].

In order to mitigate frequency stability issues, it is necessary to know the limit of wind and PV generation allowed by the grid. These limits are defined in [8, 9]. This limit can be increased with the introduction of energy storage systems as they can participate in primary frequency regulation as stated in [10, 11]. Frequency deviation analysis is vital for the correct operation of power systems. Several statistic and probabilistic methods, such as Monte Carlo simulations, have been used to analyze frequency deviations. These methods are used to study the variability of wind [12, 13], load variability [14], and the integration of wind power in power systems [15, 16]. An islanded power system is prone to have greater frequency issues than a larger, interconnected power system [17]. Monte Carlo simulations method has also been used to analyze the integration of wind power in isolated power systems [18, 19]. This paper proposes an algorithm based on Monte Carlo simulations to calculate an islanded power system's wind power limit using frequency deviations as the defining criterion.

METHODS AND MATERIALS

Algorithm used

In order to calculate the maximum wind and PV power penetration allowed by the grid it is necessary to consider the characteristics of the wind power and solar power generation as well as the conventional generation characteristics. The algorithm has been divided in subsystems for a better comprehension. First, the system's load data within a given time frame is introduced. Then the wind power and solar power output data are introduced, and the algorithm continues to calculate the parameters necessary to compute the system's frequency deviations as well as the maximum solar and wind power penetration allowed by the grid. These parameters include the load-damping coefficient, load variations, wind and solar power variations, the generation distribution and its equivalent regulation.

After the frequency deviation data are calculated the results are compared with the limits set by the grid code. The grid code establishes that under normal operation conditions frequency values must stay between 59.7 and 60.2 Hz for 95% of the year and between 59 and 61 Hz for 100% of the year. In case frequency deviation values are outside the regulated bounds an energy storage system (ESS) supports the system by providing active power support according to its rated power. If the results comply with the grid code limits, then solar and wind power contributions to the grid are increased and the algorithm is simulated again. If the end results do not comply with the grid code limits, then the last complying values for solar and wind power are set as the maximum power penetration allowed by the power system. The discussed algorithm's block diagram is depicted in figure 1.

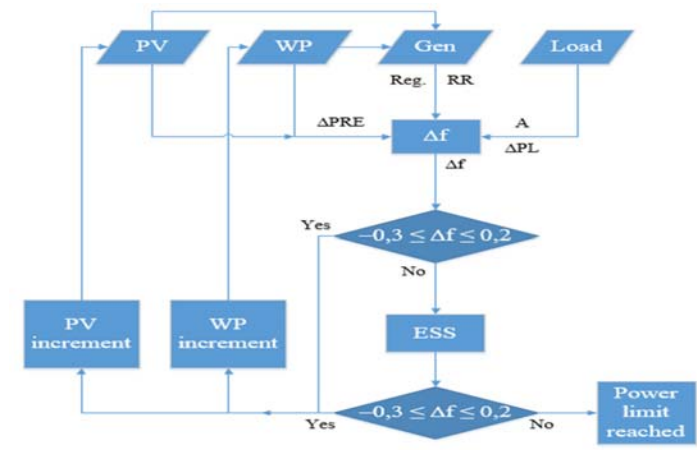


Fig. 1. Used algorithm's block diagram

Load model

The load data correspond to hourly measurements within a year's course and are stored in spreadsheet format. Loads in power systems are comprised of different types. Some are independent from the system's frequency value, such as resistive loads. Others, such as electric motors, vary their active power as frequency varies in time. According to [20], compound loads can be defined by equation (1):

$$\Delta P_{\max} = \Delta P_L + D\Delta f \quad (1)$$

Where D is the load-damping constant, expressing a load percentage change with respect to a 1% frequency change; ΔP_L is the frequency-independent load and Δf is the frequency change. The maximum load variation is calculated using equation (2):

$$\Delta P_{\max} = k_m \sqrt{P_m} \quad (2)$$

The maximum random variation (ΔP_{\max}) is calculated using k_m , which relates the mean power (P_m) with the maximum power variation for each load value. Values for k_m relate to the analyzed time of the year and correspond to values obtained in earlier studies of the analyzed power system [21]. The output of (2) is the maximum load variation corresponding to a given load value. Using this value as limit a Normal distribution is used to obtain random values of load variation smaller than ΔP_{\max} . These values can be positive or negative, corresponding to a load increase or decrease respectively.

Wind farm model

Wind speed is modeled and calculated using Weibull's distribution using the scale and form factors that correspond to the wind farm site wind speed measurements. The calculated wind speed values are introduced in the wind turbine power curve provided for by the manufacturer resulting in the power output for each wind turbine and subsequently the wind farm. The maximum wind power variation is calculated using equation (3):

$$\Delta P_w = 0,25P_{wo} \quad (3)$$

Where ΔP_w is the maximum wind power variation and P_{wo} is the wind power output. Using the output of (3) as limit a Normal distribution is used to obtain random values of wind power variation smaller than ΔP_w . These values can be positive or negative, corresponding to a wind power generation increase or decrease respectively.

Photovoltaic farm model

The PV farm power output is modeled using a Normal distribution with its standard parameters calculated corresponding to the site measurements. The farm's output can be calculated using its power curve taking into account irradiance and cloud cover data at the site. The power curve was built using random values in order to obtain closer-to-reality values. The maximum wind power variation is calculated using equation (4):

$$\Delta P_{PV} = 0,25P_{PVo} \quad (4)$$

Where ΔP_{PV} is the maximum solar power variation and P_{PVo} is the solar power output. Using ΔP_{PV} as limit a Normal distribution is used to obtain random values of solar power variation smaller than ΔP_{PV} . These values can be positive or negative, corresponding to a wind power generation increase or decrease respectively.

Generation

In this subsystem the power system's generation values are calculated in order to obtain the necessary data needed to compute the frequency deviation. The calculation method was developed in [22]. The base of the method is the compliance with the power balance equation shown in equation (5), neglecting power losses and considering the renewables active power as a negative load due to their non-dispatchable characteristics.

$$\sum P_G = \sum P_d - \sum P_{Re} \quad (5)$$

Where P_G , P_d y P_{Re} represent the generated active power, load active power and renewables active power respectively. A generation dispatch is required to satisfy equation (5). Each generating unit is limited by its designed maximum and minimum power output. These constraints are defined in equation (6).

$$P_{i,\min} \leq P_i \leq P_{i,\max} \quad \forall i \in NG \quad (6)$$

Where $P_{i,\min}$ is the generating unit i minimum output power, $P_{i,\max}$ is the generating unit i maximum output power y NG is the amount of generating units in the analyzed power system. In order to supply the demand (excluding renewables) the sum of the operation costs curves is calculated using equations (7) and (8).

$$\min \sum_{i=1}^{NG} C_i \quad (7)$$

$$C_i(P_i) = \alpha i + \beta_i P_i + \gamma_i P_i^2 \quad (8)$$

Where C_i is the operation cost of generating unit i . Variables αi , β_i , γ_i correspond to cost constants for generating unit i . After obtaining the generation distribution the algorithm calculates the regulation ranges (RR) for the primary regulation generators. The equivalent regulation (R_{eq}) is also calculated. Equations (9), (10) and (11), are used to perform these calculations.

$$RR1 = P_{i,\max} - P_i \quad (9)$$

$$RR2 = P_i - P_{i,\min} \quad (10)$$

$$R_{eq} = \frac{1}{\frac{1}{R_1} + \frac{1}{R_2} + \dots + \frac{1}{R_n}} \quad (11)$$

Where n is the amount of primary regulation generators.

According to [21] each generator's regulation is calculated using equations (12) and (13):

$$R_{p.u.} = \frac{\text{Change of frequency in p.u.}}{\text{Change of generated power in p.u.}} \quad (12)$$

$$R_{p.u.} = \frac{\frac{f_n - f_0}{f_B}}{\frac{P_G}{P_B}} \quad (13)$$

Where R_{pu} is the per-unit regulation characteristic, f_0 is the frequency at no-load, f_n is the frequency at rated power and f_B and P_B are the base frequency in Hz and MW respectively*

Frequency deviation calculation

After computing the necessary data, frequency deviation (Δf) values are calculated using equations (14) and (15).

$$\Delta f = \frac{-\Delta P_T}{\sum \frac{1}{R_{eq}} + D} \quad (14)$$

$$\Delta f = \frac{-\Delta P_T}{\sum \frac{1}{R_{eq}} + D} - \frac{\Delta P_T - RR}{D} \quad (15)$$

Where ΔP_T corresponds to the total system power variations, including load and renewables. At this point in the algorithm, if the regulation range covers any power variations, then equation (14) is used. If power variations are greater than the regulation range, then equation (15) is used instead.

Energy Storage System model

An energy storage system is introduced in the system to support its response to frequency variations in case these are out of bounds. Equation (16).

$$\Delta f = \frac{-\Delta P_T + P_{ESS}}{\sum \frac{1}{R_{eq}} + D} \quad (16)$$

Where P_{ESS} is the energy storage system power output. If the frequency deviations do not comply with the grid code limits then the ESS is used to supply the active power needed in order to keep the frequency within its limits. This operation will be constrained by the ESS rated power. As wind and solar power penetration is increased a possible outcome is that the use of the ESS is not enough to keep the frequency within its designated bounds. In this case the last complying wind and solar power penetration values are established as the maximum allowed by the studied system.

Analysed power system

The studied power system has a radial configuration with five main circuits at 34.5 kV supplying power to the distribution substations. Base generation is provided by four 3.6 MW and four 3.9 MW diesel generators at different geographic locations. In order to maintain quality of service at locations situated far from the main generation sites 1.88 MW generators are installed. These generators also serve as peak power plants at maximum demand.

Figure 2, shows the system's typical daily demand curve for the summer and winter. The winter load curve presents a significant difference between minimum load and maximum load with values of 6.4 MW and 17.8 MW respectively. This difference is much less significant in the summer load curve having a 10.8 MW minimum load and 15.6 MW maximum load.

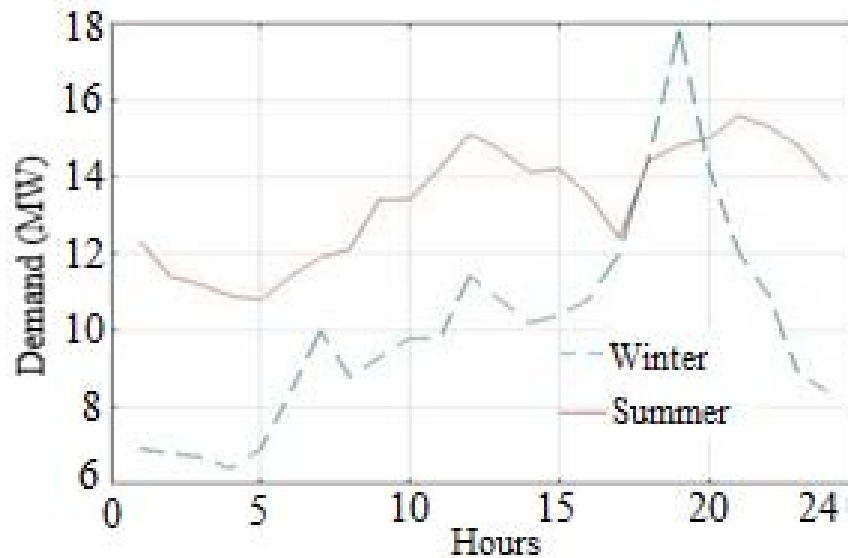


Fig. 2. Studied system's typical daily demand curve

Another important difference between the summer and winter demand curves is the load ramping, with much faster ramping in the winter. However, since the studied system's generation is diesel-based, it has a fast enough response so there are no considerable power mismatches between demand and generation. Figure 3, shows how the load is covered per generator type. The base load is covered by the 3.6 MW and the 3.9 MW diesel generators, with the 1.88 MW generators working only in the demand peaks. This load coverage was calculated using an optimization algorithm that is based on an economic pre-dispatch.

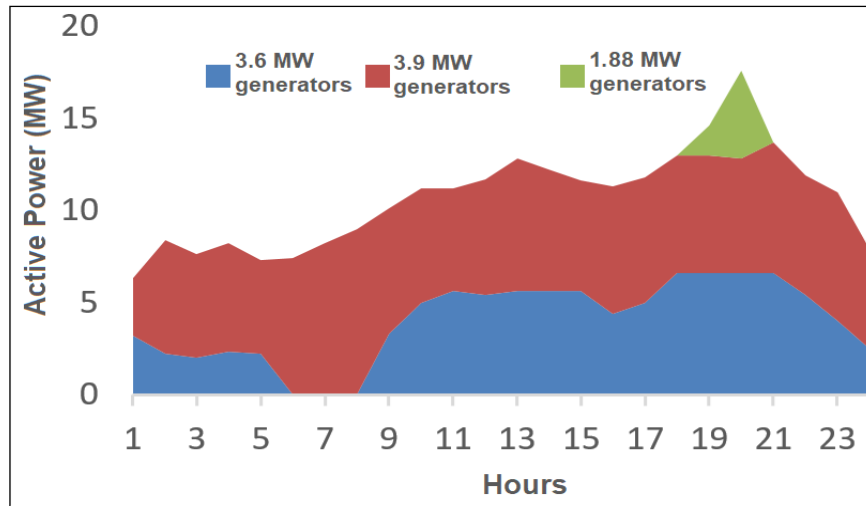


Fig. 3. Load coverage per generator type

The frequency deviation is calculated without any renewables connected to the power system. The frequency deviation histogram is shown in figure 4. The most repeated value was 0 Hz comprising a 21.2% of the total amount. There are 18 out-of-bounds values, representing the 0.02% of the total, corresponding to a correct system behavior as the out-of-bounds values are well below the permitted 5%.

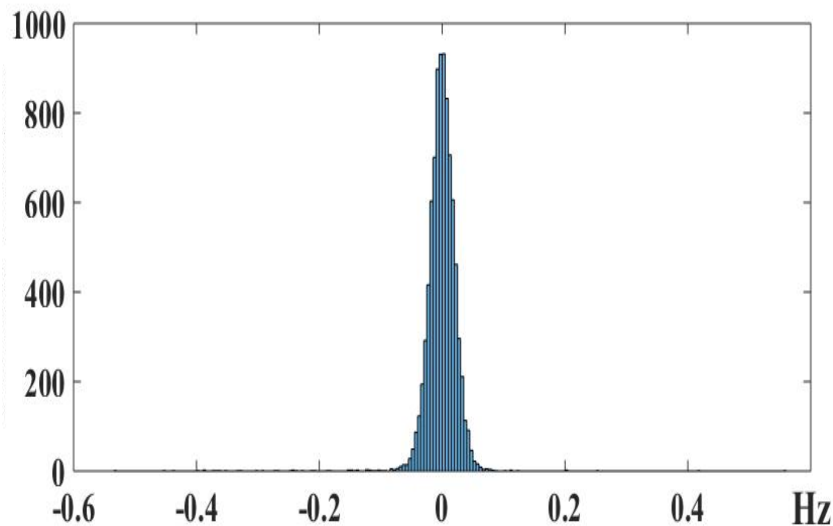


Fig. 4. Frequency deviation histogram without renewables

RESULTS AND DISCUSSION

Among the most important analyzes that must be carried out to verify that the system maintains its frequency within the regulated limits. Being vital the characterization of the system, its regulation, power reserve, and its behavior with different scenarios of integration of renewable sources. To achieve the target of 24% of penetration but maintaining the frequency within the limits established by the Cuban standard.

Renewables penetration and emission reduction assessment

Four study cases with different combinations of renewables, ESS and conventional generation were analyzed. All the scenarios include conventional generation. Figure 5, shows the penetration levels per study case. The lowest penetration values correspond to the wind-only case and the highest value corresponds to the combination of wind, PV and an ESS. As more renewables are installed in the system the fuel consumption is reduced and therefore CO₂ emissions are lower. Figure 6, shows the values for the non-spent fuel and CO₂ emission reduction per study case.

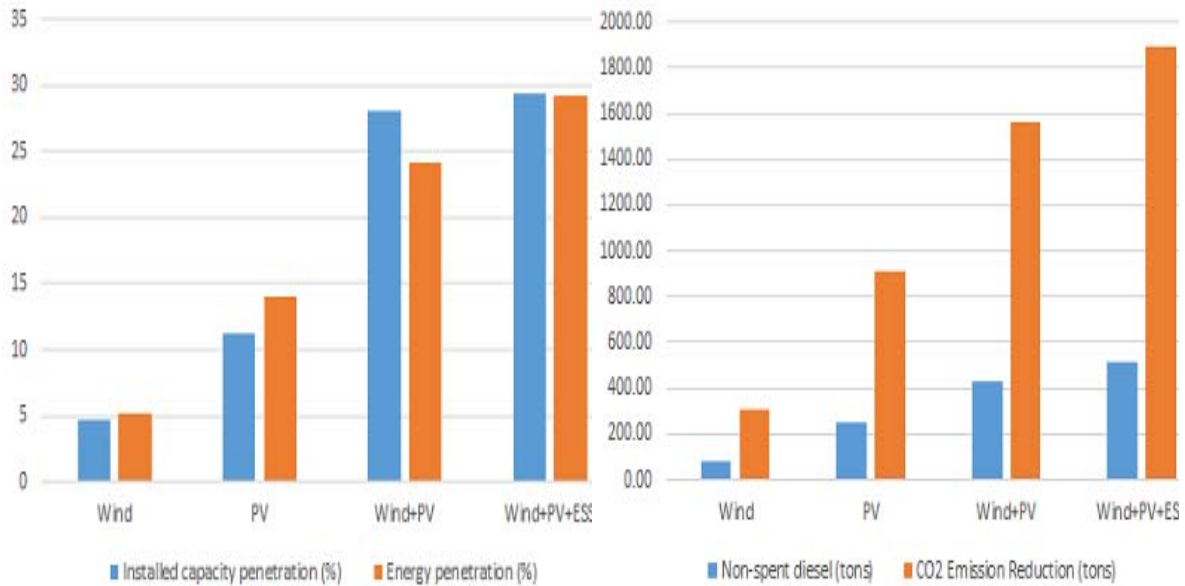


Fig. 5. Renewables penetration levels per study case

Fig. 6 Non-spent fuel and CO₂ emission reduction

Conventional generation and wind power

Figure 7, shows that there are two values outside the established limits, representing a 0.27% of the total. The most repeated values are within the limits, with 0 Hz representing a 17.43% of the total. This behavior is considered correct for this system as out of bounds values represent less than 5% of the total.

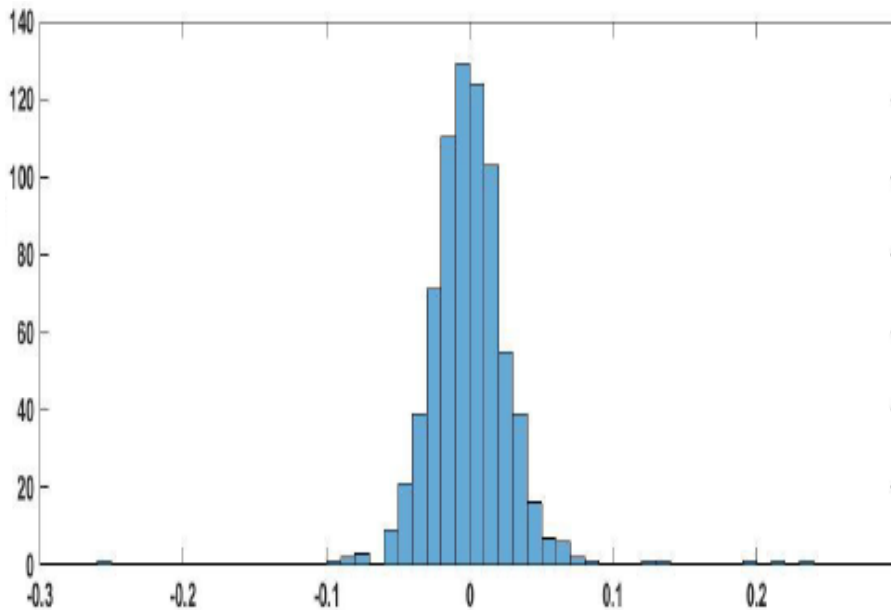


Fig. 7. Frequency deviation histogram for 1.65 MW wind power installed capacity

This scenario deals with the installation a wind power plant in the described power system. The algorithm was run several times resulting in a 1.65 MW wind power plant as the adequate solution.

Conventional generation and solar power

This scenario deals with the installation a solar power plant in the described power system. The most repeated values are within the limits, with 0 Hz representing a 36.9% of the total. Out-of-bounds values represent a 0.46% of the total. Hence the system's behavior complies with the established grid code. This scenario histogram is shown in figure 8.

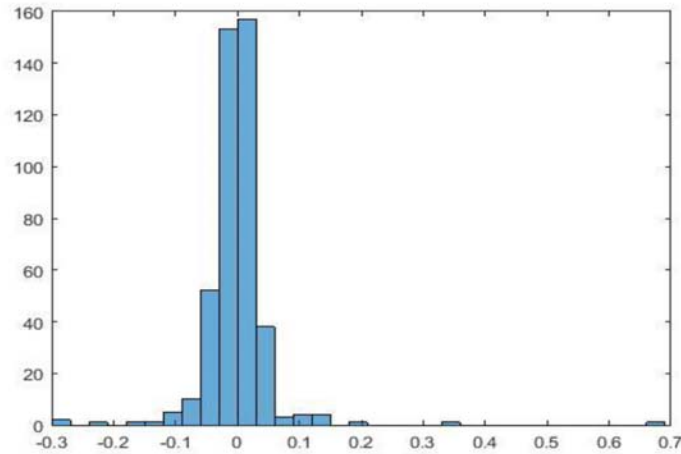


Fig. 8. Frequency deviation histogram for 4 MW solar power installed capacity

Conventional generation, wind power and solar power

This scenario deals with the installation a solar power plant and a wind power plant in the described power system. The algorithm was run several times resulting in a 4.5 MW wind power plant and a 5.5 MW solar power plant. This scenario histogram is shown in figure 9.

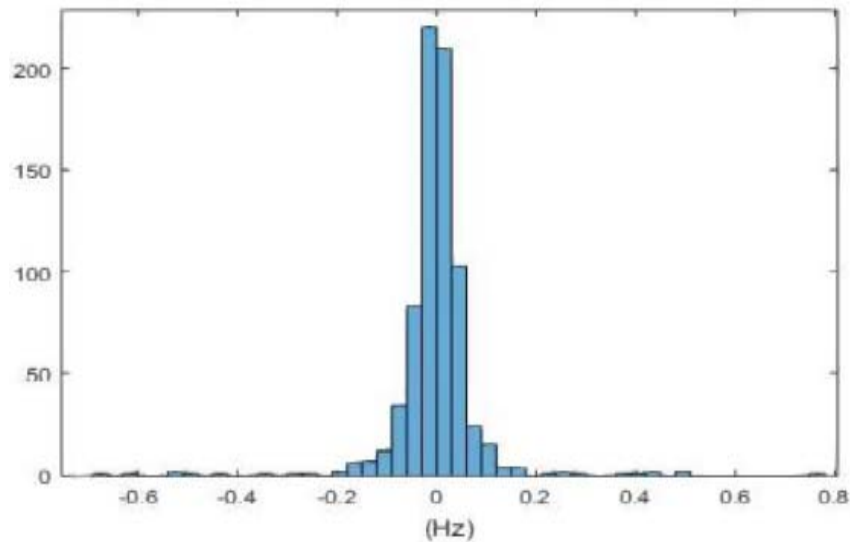


Fig. 9. Frequency deviation histogram for 4.5 MW wind power and 5.5 MW solar power installed capacity

The percentage of frequency deviation values above 0.2 Hz and below -0.3 Hz was 2.42%, below the established 5%.

Conventional generation, wind power, solar power and energy storage system

This scenario deals with the installation a solar power plant and a wind power plant in the described power system. The algorithm was run several times resulting in a 5 MW wind power plant, a 5.5 MW solar power plant and a 1 MW energy storage system. The percentage of values within the specified limits is 97.04% with no value above or below 1 Hz. This scenario histogram is shown in figure 10.

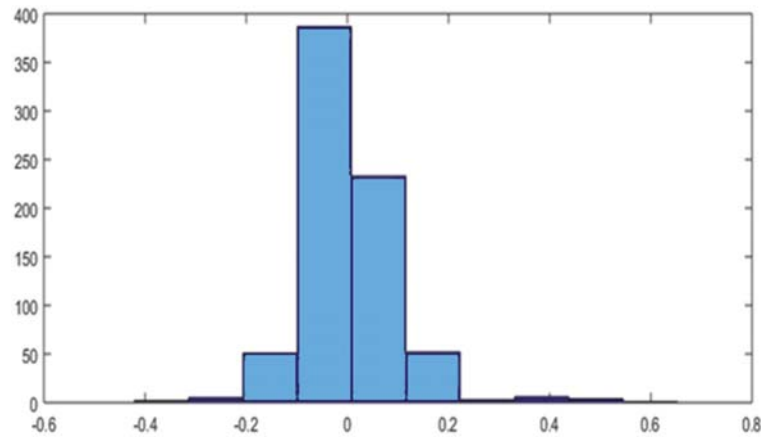


Fig. 10. Frequency deviation histogram for 5 MW wind power, 5.5 MW solar power installed capacity and a 1 MW ESS

CONCLUSIONS

A Monte-Carlo-based algorithm was developed to determine the renewable energy sources power limit by calculating the frequency deviations of an isolated power system. The algorithm was run taking into account several scenarios of an isolated power system with different wind and solar power installed capacity values. Conventional generation was considered connected in all scenarios. As expected, frequency deviations increased as the wind and solar power penetration was increased due to the reduction of the conventional generation's regulation capacity. It was found that when wind and solar work simultaneously, frequency deviations decrease due to the net wind and solar power variations leveling out each other. Also, installing an ESS allowed to increase the system's renewables power limit due to its capacity to absorb power variations whether it was generating power or using the excess power in the grid to charge itself. Future works will consider the use of using active power reserve by wind farms. This reserve will be optimized in order to maximize the wind farms energy penetration.

REFERENCES

- [1] Murdock, Hannah E., *et al.* "Renewables 2021 Global Status Report". Renewables 2021. vol. 52, n. 1. Disponible en: https://inis.iaea.org/search/search.aspx?orig_q=RN:52059346
- [2] Pairo, H. and Shoulaie, A. "Effective and simplified method in maximum efficiency control of interior permanent magnet synchronous motors". *IET Electr. Power Appl.* 2017, vol. 11, n. 3, p. 447–459. Disponible en: <https://ietresearch.onlinelibrary.wiley.com/doi/epdf/10.1049/iet-epa.2016.0617>
- [3] Fernández-Guillamón, A., *et al.* "Offshore Wind Power Integration into Future Power Systems: Overview and Trends". *Journal of Marine Science and Engineering*. 2019, vol. 7, n. 11. Disponible en: <https://www.mdpi.com/2077-1312/7/11/399/html>
- [4] Australian Energy Market Operator (AEMO). "Black System South Australia". Final Report (2017). Disponible en: https://www.aemo.com.au/-/media/Files/Electricity/NEM/Market_Notices_and_Events/Power_System_Incident_Reports/2017/Integrated-Final-Report-SA-Black-System-28-September-2016.pdf
- [5] Yiyi, Z. and Sophie, L. "China's Renewables Curtailment and Coal Assets Risk Map". *Clim. Work. Found.* (2017). Disponible en: https://data.bloomberglp.com/bnef/sites/14/2017/10/Chinas-Renewable-Curtailment-and-Coal-Assets-Risk-Map-FINAL_2.pdf
- [6] EIRGRID & SONI. "Annual Renewable Energy Constraint and Curtailment Report". (2017). Disponible en: <https://rise.esmap.org/data/files/library/ireland/RE%20Documents/RE%202011.5%20Annual-Renewable-Constraint-and-Curtailment-Report-2016-v1.0.pdf>
- [7] Roberts, C. "Review of International Grid Codes". Energy Analysis and Environmental Impacts Division Lawrence Berkeley National Laboratory. U. S. 2018. Disponible en: <https://escholarship.org/uc/item/5sv540qx>
- [8] Santos-fuentefria, A., Fernández, M. C. and García, A. M. "A new method for wind power limit calculation using P-V curves and continuation power flow routine". *Revista Cubana de Ingeniería*. 2020. vol. 11, n. 2, p. 49-57. Disponible en: <https://rci.cujae.edu.cu/index.php/rci/article/view/818/459>
- [9] Ul Abideen, M. Z., *et al.* "A Novel Methodology to Determine the Maximum PV Penetration in Distribution Networks". *2nd Int. Conf. Smart Grid Renew. Energy, SGRE 2019 - Proc.* (2019) doi:10.1109/SGRE46976.2019.9020948. Disponible en: <https://ieeexplore.ieee.org/document/9020948>

- [10] Datta, U., *et al.* "Battery Energy Storage System for Aggregated Inertia-Droop Control and a Novel Frequency Dependent State-of-Charge Recovery". *Energies* 2020, vol. 13, n. 8. Disponible en: <https://www.mdpi.com/1996-1073/13/8/2003>
- [11] Datta, U., Kalam, A. and Shi, J. "Battery energy storage system control for mitigating PV penetration impact on primary frequency control and state-of-charge recovery". *IEEE Trans. Sustain. Energy*. 2020, vol. 11, n. 2, p. 746–757. Disponible en: <https://ieeexplore.ieee.org/document/8666790>
- [12] Miao, S., *et al.* "A Markovian wind farm generation model and its application to adequacy assessment". *Renew. Energy*. 2017, vol. 113, p. 1447–1461. Disponible en: <https://www.sciencedirect.com/science/article/abs/pii/S0960148117306237>
- [13] Guo, Y. ;, Gao, H. ; and Wu, Q. "A Meteorological Information Mining-Based Wind Speed Model for Adequacy Assessment of Power Systems With Wind Power". *Int. J. Electr. Power Energy Syst.* 2017. vol. 93, p. 406–413. Disponible en: <https://www.sciencedirect.com/science/article/abs/pii/S0142061517300686>
- [14] Geng, L., Zhao, Y. and Chen, G. "Simplified Sequential Simulation of Bulk Power System Reliability Via Chronological Probability Model of Load Supplying Capability". *IEEE Trans. Power Syst.* 2018, vol. 33, p. 2349–2358. Disponible en: <https://ieeexplore.ieee.org/document/8052154>
- [15] Qiu, X., *et al.* "Reliability evaluation of power system integrated with wind farms based on control variable sampling". In *Proceedings - 2017 Chinese Automation Congress, CAC 2017* vols 2017-January p. 939–943 (Institute of Electrical and Electronics Engineers Inc., 2017). Disponible en: <https://ieeexplore.ieee.org/document/8242901>
- [16] Dui, X., Zhu, G. and Yao, L. "Two-Stage Optimization of Battery Energy Storage Capacity to Decrease Wind Power Curtailment in Grid-Connected Wind Farms". *IEEE Trans. Power Syst.* 2018, vol. 33, p. 3296–3305. Disponible en: <https://ieeexplore.ieee.org/document/8125737>
- [17] Chen, J. & Chen, J. "Stability Analysis and Parameters Optimization of Islanded Microgrid with Both Ideal and Dynamic Constant Power Loads". *IEEE Trans. Ind. Electron.* 2018, vol. 65, p. 3263–3274. Disponible en: <https://ieeexplore.ieee.org/abstract/document/8049321>
- [18] Vicente, W. C. B., Caire, R. and Hadjsaid, N. "Stochastic simulations and stability to determine maximum wind power penetration of an island network". *IEEE Power Energy Soc. Gen. Meet.* 2018-Janua, 1–5 (2018). Disponible en: <https://hal.archives-ouvertes.fr/hal-01809938/document>
- [19] Genikomsakis, K. N., *et al.* "Simulation of Wind-Battery Microgrid Based on Short-Term Wind Power Forecasting". *Appl. Sci.* 7, 2017, vol. 7, n. 11. Disponible en: <https://www.mdpi.com/2076-3417/7/11/1142/htm>
- [20] Kundur, P., Balu, N. J. and Lauby, M. G. "Power system stability and control". (McGraw-Hill, 1994). Disponible en: <https://www.accessengineeringlibrary.com/content/book/9781260473544>
- [21] Guerra, L., *et al.* "Determinación de diapasones de potencia necesarios para el control de frecuencia en el sistema eléctrico cubano". *Ing. Energética*, 2017, vol. 38, n. 1, p. 38–44. Disponible en: <https://rie.cujae.edu.cu/index.php/RIE/article/view/100/99>
- [22] Salgado Duarte, Y., Martínez del Castillo Serpa, A. and Santos Fuentefría, A. "Programación óptima del mantenimiento preventivo de generadores de sistemas de potencia con presencia eólica". *Ing. Energética*, 2018, vol. 39, n. 3, p. 157–167. Disponible en: <https://dialnet.unirioja.es/servlet/articulo?codigo=6538764>

CONFLICT OF INTERESTS

The authors declare that there are no conflicts of interest.

AUTHORS 'CONTRIBUTION

Moises Ferrer Vallin: <https://orcid.org/0000-0002-1140-652X>

Research design, data collection. Mathematical modeling and simulation of the models. He participated in the analysis of the results, writing the draft of the article, the critical review of its content, and in the final approval.

Pablo Sánchez Yáñez: <https://orcid.org/0000-0003-2645-787X>

Research design, data collection. Mathematical modeling and simulation of the models. He participated in the analysis of the results, writing the draft of the article, the critical review of its content, and in the final approval.

Ariel Santos Fuentefria: <https://orcid.org/0000-0002-9131-5539>

Research design, data collection. Mathematical modeling and simulation of the models. He participated in the analysis of the results, writing the draft of the article, the critical review of its content, and in the final approval.